Simulation of the mixture flow over terrain wave

Martin Kyncl[1,*], *Jan*Česenek[1], and *Jaroslav* Pelant[1]
[1]VZLÚ - Czech Aerospace Research Centre, Beranových 130, 199 05 Praha - Letňany, Czech Republic

Abstract. We work with the system of equations describing the non-stationary compressible turbulent multi-component flow in the gravitational field. We assume the mixture of perfect inert gases. The flow over rough terrain is simulated with the use of the finite volume method. The modified Riemann problem is solved at the boundary faces. The roughness of the surface is simulated using the alteration of the specific dissipation at the wall, and with the use of the wall functions. Velocity profile is compared with the experimental results. Own-developed computational code is used.

1 Introduction

Our aim is to numerically simulate the flow of the perfect gas mixture. We consider the viscous compressible gas flow, described by the Reynolds- Averaged Navier-Stokes equations with the k-ω model of turbulence. This system is equipped with the equation of state in more general form, and with the mass conservation of the additional gas specie. The expected result is to construct a method suitable for the estimates of the pollutant concentrations caused by the given source. This contribution follows previous work [1–4].

2 Formulation of the Equations

We consider the conservation laws for viscous compressible turbulent flow of ideal gas with the zero heat sources in a domain $\Omega \in \boldsymbol{R}^N$, and time interval $(0,T)$, with $T > 0$. The system of the Reynolds-Averaged Navier-Stokes equations in 3D has the form

$$\frac{\partial \boldsymbol{w}}{\partial t}+\sum_{s=1}^{3}\frac{\partial \boldsymbol{f}_s(\boldsymbol{w})}{\partial x_s}=\sum_{s=1}^{3}\frac{\partial \boldsymbol{R}_s(\boldsymbol{w},\nabla \boldsymbol{w})}{\partial x_s}+\boldsymbol{S} \quad \text{in } Q_T=\Omega\times(0,T). \tag{1}$$

Here x_1, x_2, x_3 are the space coordinates, t the time, $\boldsymbol{w} = \boldsymbol{w}(x,t) = (\varrho, \varrho v_1, \varrho v_2, \varrho v_3, E)^T$ is the state vector, $\boldsymbol{f}_s = (\varrho v_s, \varrho v_s v_1 + \delta_{s1}p, \varrho v_s v_2 + \delta_{s2}p, \varrho v_s v_3 + \delta_{s3}p, (E+p)v_s)^T$ are the inviscid fluxes, $\boldsymbol{R}_s = (0, \tau_{s1}, \tau_{s2}, \tau_{s3}, \sum_{r=1}^{3}\tau_{sr}v_r + C_k\partial\theta/\partial x_s)^T$ are the viscous fluxes, $\boldsymbol{S}$ are additional sources. $\boldsymbol{v} = (v_1, v_2, v_3)^T$ denotes the velocity vector, ϱ is the density, p the pressure, θ the absolute temperature, $E = \varrho e + \frac{1}{2}\varrho\boldsymbol{v}^2$ the total energy. Further $\tau_{ij} = (\mu+\mu_T)S_{ij} - \delta_{ij}\frac{2}{3}\varrho k$, with $S_{11} = \frac{2}{3}\left(2\frac{\partial v_1}{\partial x_1} - \frac{\partial v_2}{\partial x_2} - \frac{\partial v_3}{\partial x_3}\right), S_{12} = \frac{\partial v_1}{\partial x_2} + \frac{\partial v_2}{\partial x_1}, S_{13} = \frac{\partial v_1}{\partial x_3} + \frac{\partial v_3}{\partial x_1}, S_{21} = S_{12}, S_{22} = \frac{2}{3}\left(-\frac{\partial v_1}{\partial x_1} + 2\frac{\partial v_2}{\partial x_2} - \frac{\partial v_3}{\partial x_3}\right), S_{23} = \frac{\partial v_2}{\partial x_3} + \frac{\partial v_3}{\partial x_2}, S_{31} = S_{13}, S_{32} = S_{23}, S_{33} = \frac{2}{3}\left(-\frac{\partial v_1}{\partial x_1} - \frac{\partial v_2}{\partial x_2} + 2\frac{\partial v_3}{\partial x_3}\right)$, where μ is the dynamic viscosity coefficient dependent on temperature, μ_T is the eddy-viscosity coefficient. For the specific internal energy $e = c_v\theta$ we assume the caloric equation of state $e = p/\varrho(\gamma-1)$, c_v is the specific heat at constant volume, $\gamma > 1$ is called the *Poisson adiabatic constant*. The constant C_k denotes the heat conduction coefficient $C_k = (\frac{\mu}{P_r} + \frac{\mu_T}{P_{r_T}})c_v\gamma$, and P_r is laminar and P_{r_T} is turbulent Prandtl constant number. In our application of flow in the gravitational field we set the source terms to $\boldsymbol{S} = (0, \varrho g_1, \varrho g_2, \varrho g_3, \varrho\boldsymbol{g}\cdot\boldsymbol{v})$, where $\boldsymbol{g} = (g_1, g_2, g_3)$ is the gravity vector. For the gas mixture with two species we use the Dalton's law for the total mixture pressure

$$p = p_1 + p_2,$$

where p_1 and p_2 are the partial pressures of the first and second component gas. Let ϱ_1 and ϱ_2 be the mass density of these components. Then the total mass density of mixture is

$$\varrho = \varrho_1 + \varrho_2.$$

Temperature θ is same for all gases in the mixture, and the equation of state holds

$$p_i = \varrho_i R_i\theta, \quad R_i = \frac{R_g}{m_i},$$

where $R_g = 8.3144621$ is universal gas constant, and m_i denotes the mollar mass of the ith specie. We can introduce the species mass fractions Y_1, Y_2, with $Y_1 = \frac{\varrho_1}{\varrho}, Y_2 = \frac{\varrho_2}{\varrho}$, it is $Y_1 + Y_2 = 1$. The thermodynamic constants of the mixture satisfy (using the decomposition of the internal specific energy and enthalpy)

$$\varrho c_p = \sum \varrho_i c_{pi}, \quad \varrho c_V = \sum \varrho_i c_{Vi},$$

then the adiabatic constant γ, needed in the solution of (1), can be written as

$$\gamma = \frac{c_p}{c_V} = \frac{\sum Y_i c_{pi}}{\sum Y_i c_{Vi}}.$$

*e-mail: kyncl@vzlu.cz

The system (1) is then extended with the conservation law of the mass for one gas component (specie)

$$\frac{\partial \varrho Y_1}{\partial t} + \frac{\partial \varrho Y_1 v_1}{\partial x_1} + \frac{\partial \varrho Y_1 v_2}{\partial x_2} + \frac{\partial \varrho Y_1 v_3}{\partial x_3} = \frac{\partial}{\partial x_1}\left(\sigma_C \mu_T \frac{\partial Y_1}{\partial x_1}\right) + \frac{\partial}{\partial x_2}\left(\sigma_C \mu_T \frac{\partial Y_1}{\partial x_2}\right) + \frac{\partial}{\partial x_3}\left(\sigma_C \mu_T \frac{\partial Y_1}{\partial x_3}\right). \quad (2)$$

Here σ_C is diffusion coefficient. The mass conservation for the second specie is automatically satisfied via the system (1).

Here we assume the system (1),(2) equipped with the two-equation turbulent model $k-\omega$ (Kok), described in [5].

3 Numerical method

For the discretization of the system we proceed as described in [6–8]. We use either explicit or implicit finite volume method (FVM) to solve the systems (1), (2) sequentionally. Other possible discretizations were shown in [9, 10]. The used FVM discretizations were presented in [4], we use the Riemann solver [11] for system (1), and Vijayasundaram numerical flux in (2).

4 Example: 3D diffusion of the passive mixture

Here we present a simple case for the test of the used numerical method. Let us assume the stationary flow with $\boldsymbol{v} = (0,0,0)$, and with constant $\sigma = \frac{\sigma_C \mu_T}{\varrho} = 1$. Let us solve the problem (2) with the boundary condition

$$\nabla Y_1 \cdot \boldsymbol{n} = 0,$$

and initial condition given at time $t_0 = 0.001\ s$

$$Y_1(x_1, x_2, x_3, t_0) = \frac{1}{8\ (\pi\ \sigma\ t_0)^{3/2}}\ \exp\left(-\frac{x_1^2 + x_2^2 + x_3^2}{4\sigma t_0}\right),$$

The analytical solution is known and it can be written as

$$Y_1(x_1, x_2, x_3, t) = \frac{1}{8\ [\pi\ \sigma\ (t + t_0)]^{3/2}}\ \exp\left(-\frac{x_1^2 + x_2^2 + x_3^2}{4\sigma(t + t_0)}\right).$$

The figure 1 shows computational results for unit domain, and comparison with analytical solution.

5 Example: the flow over terrain wave

We chose to simulate the flow over the rough terrain with the sinus wave geometry, accordingly to experiments shown in [12]. Lenght of the wave was set to 0.800 m, height to 0.114 m. The experimental work was done in the boundary layer wind tunnel (BLWT) in VZLU,a.s. The test section for boundary layer development was 13.6 m long. The boundary layer developed over the entire test section with plastic sheet with high truncated cones 7mm high and a rectangular barrier 140 mm high, which served as turbulence generator. The horizontal velocity profile $U(y)$ in the start of the test section corresponds with its typical logarithmic shape estimated by the law of the wall (see [3, 5])

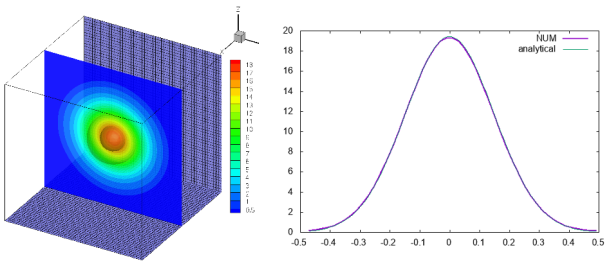

Fig. 1. 3D diffusion: simulation and comparison with the analytical solution at time $t = 0.01\ s$, x_1-cut through the center.

$$U(y)/u_\tau = \frac{1}{\kappa} ln(\frac{y}{z_S} + 1), \quad (3)$$

where z_S is the wall roughness, y denotes vertical coordinate, and u_τ is the friction velocity, $\kappa \approx 0.41$ (Karman's constant). The example of measured velocity profiles is shown in figure 2. The least squares method was used for the estimation of the values for u_τ and z_S.

For the simulations of the compressible gas flow in the atmosphere we assume the change of variables with the vertical coordinate y. We use the following initial conditons for the horizontal velocity component u, temperature θ, pressure p, density ϱ

$$\theta_0 = \theta_{00} - 0.0065y,$$
$$p_0 = p_{00}\left(1 - \frac{0.0065}{\theta_{00}}y\right)^{\frac{g}{-0.0065R}}, \quad g = -9.81,$$
$$u(y) = min\left(\frac{u_\tau}{\kappa} log(\frac{y}{z_S} + 1), u_\infty\right),$$
$$\theta = \theta_0\left(1 - \frac{\gamma - 1}{2}\frac{u^2}{\gamma R \theta_0}\right),$$
$$p = p_0\left(\frac{\theta}{\theta_0}\right)^{\frac{\gamma}{\gamma - 1}},$$
$$\varrho = p/(R\theta).$$

Here θ_0 denotes total temperature, p_0 total pressure, $\theta_{00} = 293.15\ K$ is the chosen total temperature and $p_{00} = 101325\ Pa$ total pressure at $y = 0\ m$, $u_\infty = 10\ m \cdot s^{-1}$ is chosen velocity regime, and $R = 287.04\ J \cdot kg^{-1} \cdot K^{-1}$ is the gas constant. Here we used the law of wall and the adiabatic approximations for perfect gas.

In order to to get the state variables at each boundary face we solve the local boundary problem with the use the original analysis of exact solution of the Riemann problem. This approach was shown and described in [13, 14] and analyzed also in [8], [15–17]. Using the thorough analysis of the Riemann problem we have shown, that the missing initial condition for the local problem can be partially replaced by the suitable complementary conditions. We suggest such complementary conditions accordingly to

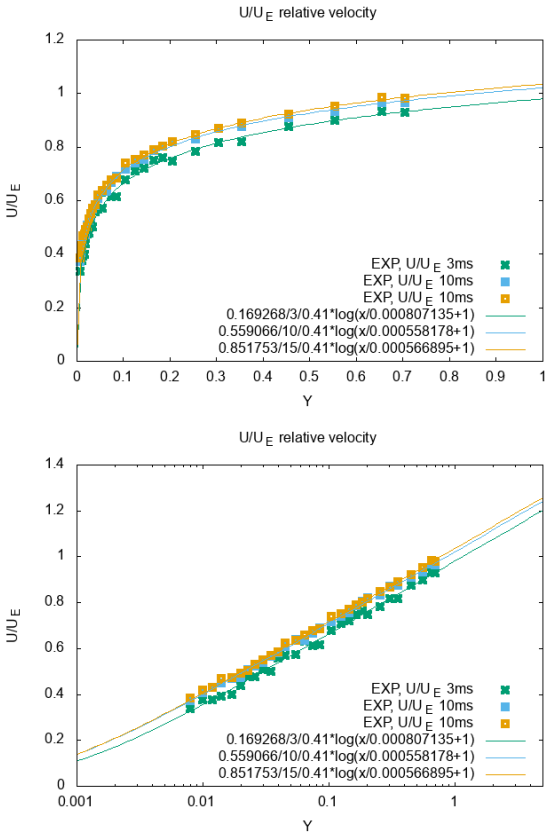

Fig. 2. The flow over rough plate: measured relative velocity profile, and estimate by the logatithmic profile $U(y)/u_\tau = \frac{1}{\kappa} log(\frac{y}{z_S} + 1)$. Constants u_τ, z_S were computed using the least-squares approximation of measured data. Velocity regimes $U_E = 3\ m \cdot s^{-1}, 10\ m \cdot s^{-1}$ and $15\ m \cdot s^{-1}$.

the desired preference. This way it is possible to construct the boundary conditions by the preference of total values, by preference of pressure, velocity, mass flow, temperature. On the contrary to the initial-value Riemann problem, the solution of such modified problems can be written in the closed form for some cases. Moreover, using such construction, the local conservation laws are not violated. Here we used the boundary conditions by preference of known velocity at the outlet, as described in [13, 15]. This boundary condition was modified at the inlet by adding the known (estimated) total temperature, shown above.

For the simulation of the rough wall we use either the modification of the specific turbulent dissipation ω or the so-called **wall functions** for the estimation of values at the first cell (near wall). We estimate the friction velocity u_τ, assuming the law of the wall (see [3, 5]) to be valid at the closest volume, i.e. solve the equation

$$U_P/u_\tau = \frac{1}{\kappa} ln(\frac{y_P}{z_S} + 1),$$

where U_P is the horizontal velocity at the considered cell, and y_P denotes the cell center distance from surface. The wall friction $\tau_w = \mu \frac{\partial U}{\partial y}|_w$ is then estimated as $\tau_w = \varrho_w u_\tau^2$.

The momentum equations are solved with the modified effective viscosity μ_e at the wall: $\mu_e \frac{U_P}{y_P} = \tau_w$. The values for the k, ω at the first cell are set using log layer equations

$$k_P = \frac{u_\tau^2}{\sqrt{\beta^*}},\ \omega_P = \frac{u_\tau}{\sqrt{\beta^*}\kappa y_P}.$$

We use further modifications of this wall function shown in [4] in order to avoid the problem with possible zero velocity U_P.

The regime constants for the considered flow above the rough terrain wave were chosen as

$$u_\infty = 10\ m \cdot s^{-1},$$

$$z_S = 0.000558178\ m,$$

$$p_{00} = 101325\ Pa,$$

$$\theta_{00} = 293.15\ K.$$

The friction velocity forming the initial condition was set to $u_\tau = 0.559066\ m \cdot s^{-1}$. The figure 3 shows computed velocity profiles together with the experimentally obtained results.

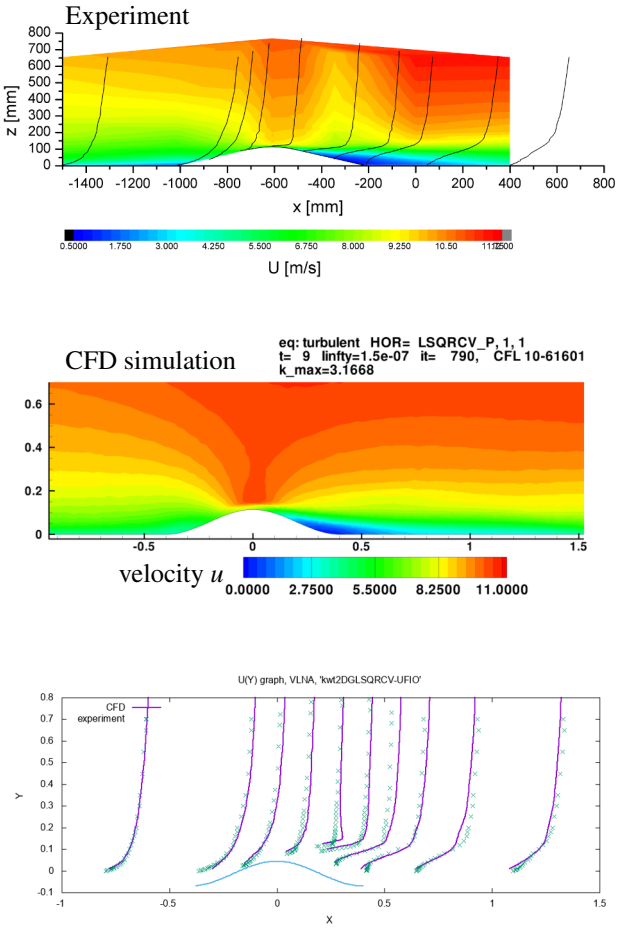

Fig. 3. The flow over the terrain wave: measured horizontal velocity profile at given vertical lines, and numerical simulation. Direct comparison is shown in the bottom picture.

Further we simulated dispersion of the gas mixture. The emmision source was located at the top of the wave,

on winward and on leeward side. The source was simulated using marked air with chosen mass fraction $Y_1 = 0.1$ at the chosen elements. The computed results are shown in figure 4.

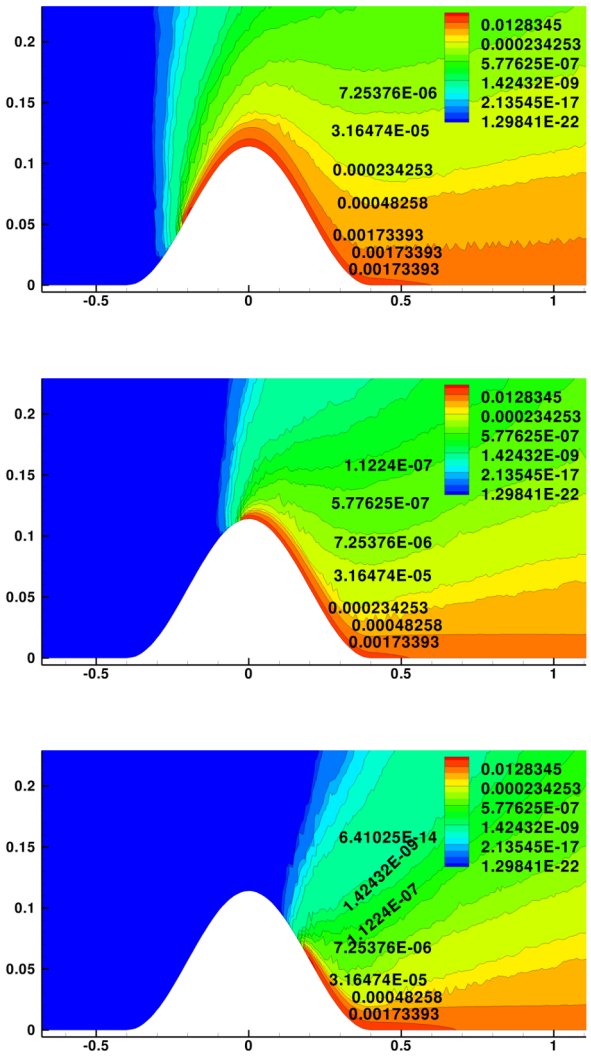

Fig. 4. The flow over the terrain wave: numerical simulation, mass fraction Y_1 of the emmision for various source placement.

Conclusion

This paper is focused on the numerical simulation of the mixture of two inert perfect gases in the gravitational field. The finite volume method is applied for the solution of the system of equations. The modification of the Riemann problem and its solution was used at the boundaries. All codes were implemented into the own-developed software. The numerical examples of the flow above the rough surface simulating terrain wave were presented.

Acknowledgements. The results originated with the support of Ministry of the Interior of the Czech Republic, project VI20172020092 - Simulation of fire and smoke dispersion in critical infrastructure area in case of accident or aircraft attack, project SCENT, Grant MSM 0001066902 of the Ministry of Education of the Czech Republic, and Ministry of Industry and Trade of the Czech Republic for the long-term strategic development of the research organization. The authors acknowledge this support.

References

1. M. Kyncl and J. Pelant, *EPJ WoC*, **114**, 02064, (2016)
2. M. Kyncl and J. Pelant, *ENGINEERING MECHANICS 2016*, **22**, p.367-370, (2016)
3. M. Kyncl and J. Pelant, *EPJ WoC*, **92**, 02044, (2015)
4. M. Kyncl and J. Pelant, *EPJ WoC*, **213**, 02050, (2019)
5. C. J. Kok, *AIAA Journal*, **38**, 7, (2000)
6. M. Feistauer, J. Felcman, and I. Straškraba, *Mathematical and Computational Methods for Compressible Flow*. Oxford University Press, Oxford, (2003)
7. M. Kyncl and J. Pelant, *Implicit method for the 3d RANS equations with the k-ω (Kok) Turbulent Model.* Technical report R5453, (2012)
8. M. Kyncl and J. Pelant, *Implicit method for the 3d Euler equations.* Technical report R5375, VZLÚ, (2012)
9. J. Česenek, *EPJ WoC* **114**, 02012 (2016)
10. J. Česenek, *EPJ WoC* **180**, 02016 (2018)
11. E. F. Toro, *Riemann Solvers and Numerical Methods for Fluid Dynamics*. Springer, Berlin, (1997)
12. P. Michálek and D. Zacho, *EPJ WoC*, **92**, 02051, (2015)
13. M. Kyncl and J. Pelant, *EPJ WoC*, **143**, 02061, (2017)
14. M. Kyncl and J. Pelant, *Proc. ECCOMAS 2016, 5.-10.6.2016*, Greece (2016)
15. M. Kyncl. *Numerical solution of the three-dimensional compressible flow.* Doctoral Thesis, Prague, (2011)
16. M. Kyncl and J. Pelant, *Proc. ECCOMAS 2014, ECFD VI, 20.-25.7.2014*, Spain (2014)
17. M. Kyncl and J. Pelant, *Appl. Mech. and Mat.*, **821**, 70-78, (2016)